Development of an UAV with Application of Topology Optimization for 3D Printing

Ricardo Gaspar Esteves Teixeira da Costa
ricardo.teixeira.costa@tecnico.ulisboa.pt

Instituto Superior Técnico, Universidade de Lisboa, Portugal

September 2021

Abstract

The applicability of the Additive Manufacturing (AM) methods has undergone an exponential growth over the last years and, along with the Topology Optimization (TO) field, has allowed introducing innovations and improvements in several engineering fields. Taking advantage of these technological advances, the conceptual design and development of a small unmanned aircraft was carried out, with the objective of applying these more advanced and modern methods to its study and production, in order to make the whole development and manufacturing process more efficient. Prior to the application of the topology optimization process, a standard aircraft development methodology was carried out, with selection of geometries, configurations and aerodynamic studies. This was followed by a TO, a computational tool that allows the design of lighter structures, without compromising their structural integrity. In the case of this work, its use is aimed at optimizing the aircraft fuselage, from the point of view of the amount of material used and, consequently, its mass, but capable of dealing with the most critical aerodynamic loads. For this purpose, the critical loads obtained from Computational Fluid Dynamics simulations for the limits of the flight envelope will be considered. All the aircraft's internal components are also taken into account, from instrumentation to wiring and propulsion system, both for the loads they impose and for their accommodation. The resulting design can then be post-processed for manufacturing using an AM technology such as Fused Deposition Modeling (FDM).

Keywords: Topology Optimization, Additive Manufacturing, Computational Fluid Dynamics, Aircraft Design, Unmanned Aerial Vehicle.

1. Introduction

We live in times where any person with some knowledge and a moderate computing power, can perform analysis and optimization tasks of various parameters, within the scope of engineering projects, which a few years ago would have required an enormous effort and consumed many more resources, whether temporal, monetary or manpower.

Taking advantage of this greater ease of carrying out a development project, in this case of an aircraft, we embraced the challenge of studying and conceptually designing an unmanned aircraft, a UAV (Unmanned Aerial Vehicle) or UAS (Unmanned Aerial System) applying in its development several analysis techniques and 3D printing technology, coupled with a topology optimization, which allows to fully exploit the advantages inherent in this type of printing and production of components.

Regarding the manufacturing method chosen, 3D printing, its choice was due to the proliferation that this technology has had in recent years, both in the domestic and professional environments. In addition, it allows the creation of more optimized geometries, due to the ease with which it can create complex internal structures and, as such, remove many of the manufacturing limits applied to topology optimization studies, when combined with more traditional manufacturing processes.

Having defined the genesis of the proposed project, the time has come to give a more specific purpose to the target aircraft of the study, also as a way to impose requirements and limits to its design and performance. The need for greater visual coverage of the a racetrack, so far guaranteed only by fixed cameras distributed along the track and by the eyes of the stewards themselves, becomes, in certain circumstances, quite notorious, and the current solution does not cover all the necessary angles of vision to clarify some dubious situations.

Therefore, a set of UAVs that could fly over the runway, with a previously defined route, and keep a constant coverage of the runway activity, could be part of the solution to the problem mentioned above.

2. Methods and Tools

Behind the development of any product or component is a reason that led to its production. In this case, the desire to explore the capabilities of using topological optimization, coupled with additive manufacturing, applied to the development of an UAV.

2.1. Requirements and Initial Sizing

The function for which the aircraft will be designed, demands certain requirements that served as constraints for the con-

ceptual development of it. Among them are the need to carry a high-resolution camera, with a wide-angle lens, that allows to cover the largest possible runway area without losing image quality when approaching for incident observation, so as to reduce as much as possible the number of UAVs needed to visually cover the entire track. It is also necessary to integrate an autopilot system, so that the trajectory of the aircraft can be defined in advance and does not require constant monitoring by a pilot. Other requirements relate to the choice of a geometry that benefits a greater endurance, as well as its versatility when being launched and transported. Therefore, a flying wing configuration was chosen, as it has a high lift area and low drag values [1]. On the other hand, it requires greater care with the internal layout of the UAV, in order to control the longitudinal position of the center of gravity, and the longitudinal control of this type of aircraft is more demanding [2].

In terms of wingspan restrictions, these are related to the goal that the UAV can be hand launched by anyone. The average arm length of an adult is around 60 to 80 cm, so this was the measure selected for the half-span of the aircraft.

The initial sizing of an aircraft is one of the first steps in the aircraft development process [3, 4]. To this end, a prior choice had to be made of the internal components to be used, in order to allow a more correct prediction of the size of the fuselage and to calculate the mass of all of them, and with that, to begin the process of sizing the wings. In order to estimate a target for the UAV structural mass value, a survey of the masses of aircraft with similar configurations and wingspans was done.

The whole process below follows the normal phases of an aircraft development, according to Corke's textbook [3], with only minor adaptations taking into account the type of propulsion system and the use for which the UAV is intended.

2.2. Conceptual Design

Once the mass balance of the internal components and structure of the UAV was completed, it was then possible to calculate the Maximum Take Off Weight (MTOW) which, together with other selected flight parameters, such as cruise speed, flight altitude and corresponding air characteristics at this same altitude, allowed proceeding with the determination of the wing area and required power, using semi-empirical equations. The selection of wing loading (W/S) and power-to-weight ratio (P/W) plays a key role in the design of any aircraft, including UAVs. These two parameters not only guide flight performance, but also help determine the dimensions of the aircraft for a given set of aerodynamic and weight properties.

In order to calculate their value, and thus find the Design Point that will drive the beginning of the aircraft design, some restrictive equations were selected, each corresponding to a different flight phase or event. Right from the start, since this is an aircraft with the purpose of performing long duration and surveillance flights, the constraints of the cruise and endurance flight conditions would have to be taken into account. Additionally, the cruise flight conditions for maximum speed, climb and stall speed condition were also considered.

By obtaining the Design Point, it becomes possible to calculate the wing area (S) and the power (P) required to execute any phase of flight. With this data and the imposed wingspan (b) limitation, the geometric parameters of the wings are obtained.

2.3. Preliminary Design

2.3.1 Wing Profile Selection

Once the aircraft sizing and configuration are complete, it is time to proceed with the selection of the wing profile to be used in the wings. Due to the fact that this is a flying wing, with no horizontal stabilizer to assist in longitudinal stability, it is of utmost importance that the moment coefficient is as close to zero as possible. Based on this requirement, and based on studies done and published [5, 6], an initial selection of some possible profiles to be used was made.

The choice of the program that allowed performing aerodynamic studies on those profiles, fell on XFLR5 [7]. This software uses XFoil [8] to provide the aerodynamic coefficients of an airfoil.

In preparing the analyses some parameters were introduced, such as the Reynolds number (Re) and the range of angles of attack at which the profiles are to be subjected to analysis. Regarding the chord used, this was the average chord, calculated earlier in the initial sizing process.

Several aspects were taken into account to select the most suitable airfoil based on the obtained graphs, such as the curves C_l/C_d as a function of the angle of attack α, C_l as a function of α, C_d as a function of α and C_m as a function of α, where C_l represents the lift coefficient, C_d the drag coefficient and C_m the moment coefficient.

As far as the C_l/C_d ratio is concerned, we want higher values to increase efficiency, but also a wide range of angles of attack in which the value remains high. As for the drag coefficient (C_d), it is intended to be as low as possible, since it is directly related to the drag force present in the profile and in the aircraft, and consequently to the power required to keep the aircraft in level flight. As for the lift coefficient (C_l), we want its maximum value ($C_{l_{max}}$) to be as high as possible before entering in stall, which should not be too abrupt. Finally, the moment coefficient (C_m) is wanted as close as possible to zero and negative in the operational range of the aircraft.

2.3.2 Wing Configuration

After selecting the airfoil to be used, it was time to configure the wing. In terms of sizing, this was subject to requirements imposed by aspects such as the accommodation capacity of the servo motors and the possibility of performing take-offs by hand launching, which entails minimum or maximum values for dimensions such as wing thickness and wingspan.

Being an aircraft with the purpose of performing flights of considerable duration, privileging the endurance, there is a natural demand for obtaining a low lift induced drag. Based on this requirement, even though an elliptical shape would be more efficient from an aerodynamic perspective, its construc-

tion process would be difficult and expensive [3]. Therefore, the best compromise between aerodynamic efficiency and ease of construction led to the adoption of a trapezoidal wing.

Before moving on to the aerodynamic analysis of the wing, a number of parameters had to be defined. Starting with an intrinsic characteristic of trapezoidal wings, the taper ratio (λ), which is the ratio between the chords at the wing tip (c_{tip}) and root (c_{root}), brings about some effects, namely changing the distribution of lift on the wing, allowing it to become more elliptical. Another aspect that changes with the introduction of tapering is the position of the center of mass of each wing, tending to move closer to the fuselage, since there is less area and less material in the outer region of the wing. Consequently, the bending moment at the wing root will have less magnitude, enabling a reduction in structural weight. Ideal values for the taper ratio to minimize the lift induced drag and bring the lift distribution as close as possible to the elliptical distribution, can be consulted in the references [3, 9].

The wing sweep angle (Λ) was another parameter taken into account and studied for a better wing configuration. The lateral stability of the aircraft tends to increase with the introduction of sweep angle [10]. On the other hand, the stall speed tends to increase with the sweep angle, and for very high values, the efficiency of the wing (C_L/C_D) decreases, as well as the maximum lift coefficient. More information about the importance of the sweep angle and the most appropriate values for tailless UAVs can be found in [11].

Besides λ and Λ, also the dihedral angle (Γ) of the wing was analyzed. Low dynamic lateral stability is a problem that characterizes tailless aircraft, and this can be countered by introducing a positive dihedral on the wing.

Finally, the last parameter to take into account for a complete wing configuration is the aspect ratio (AR), which is the ratio between the wingspan squared and the wing area. If on the one hand high values lead to a greater aerodynamic efficiency, since the induced drag reduces with increasing AR, on the other hand these wings are usually associated to large wingspans that result in larger bending moments, which in turn require structural reinforcement. In [12] small UAVs are analyzed, and the most appropriate range of AR values can be consulted.

After defining the above parameters, an aerodynamic analysis on the complete aircraft is performed. First, a 2D analysis should be run for the wing and fuselage profiles, with a Reynolds number range that goes from the lowest Reynolds number verified at the wing tip, where the chord is the smallest, to the maximum value allowed by XFLR5. This range aims to encompass any values experienced in the model.

The full aircraft is then modelled in XFLR5 considering not only its dimensions but also its mass and weight distribution, a point that will be the subject of analysis in sub-chapter 2.3.3. The flow parameters, velocity (V), density (ρ), kinematic viscosity (ν) were also defined. The Lifting Line Theory [13], which consists of the superposition of horseshoe vortices along the wingspan is the method used. It has some limitations, namely the impossibility of application to multiple surfaces or asymmetric flows. Still, it already takes viscosity into account when calculating the model friction. A polar type was selected with constant speed, in this case the cruise speed, and inertial properties and reference dimensions from the aircraft configuration were introduced. It should also be noted that the study should be carried out for a range of angles of attack that encompasses all flight conditions to which the UAV is subjected.

This aerodynamic analysis provides important data about the aircraft, such as the angle of attack for cruise condition, which can be obtained by consulting the graph of C_L vs. α, having previously calculated the lift coefficient for level flight ($C_{L_{eq}}$). Having access to the α value, all the other coefficients for cruise condition can be consulted. Other relevant data that can be taken from the results of this analysis are the angle at which the aircraft stalls, in this case for its cruise speed, and the stall speed for α_{trim}, which allows to impose limits and a safety margin when programming the autopilot.

2.3.3 Static Stability Analysis

To ensure airworthiness of the proposed aircraft it is necessary to evaluate its static and dynamic stability. However, since at the early design stages only static stability is usually considered, for this work only a static stability analysis was performed on the full aircraft. This analysis was done in the XFLR5 by assessing the longitudinal stability and static margin. Longitudinal stability can be assessed by the sign of the slope C_{M_α}. If this is negative, it means that with increasing angle of attack the aircraft will experience an increasingly negative pitch moment (C_M), counteracting the unwanted increase in angle of attack and leading to stability [10]. Thus, a negative value of C_M for $\alpha = 0$ is a requirement for longitudinal stability. The static margin (K_n) plays an important role in the longitudinal stability of the aircraft. With this in mind, it is important to ensure that its value is positive. Static margin values between 0.02 and 0.08 are advised for tailless aircraft [14].

First, an initial distribution of the components inside the fuselage is made, which will be redefined after obtaining the first estimate of the static margin. Then, analyzing the graph of the moment coefficient as a function of the angle of attack, the coordinates of the neutral point, which coincides with the aerodynamic center, are taken, since it is tailless aircraft, by determining the position of the CG for which C_M is independent of α. Having found this value, one proceeds to the reposition of the internal components in order to obtain a x_{CG} coordinate that leads to a static margin within the advised range.

Directional stability should also be analyzed given the unconventional nature of the chosen design. Directional motion in an aircraft corresponds to a rotation about the vertical axis. In a flight situation, the forces that induce a yaw motion in the aircraft are lateral forces produced by the fuselage and wings, thanks to a lateral skid vector that makes a slip angle β with the longitudinal axis [3]. To ensure directional stability, the yaw moment coefficient C_{n_β} of the aircraft has

to be positive [3].

2.3.4 Flight Envelope

The last step before starting the CFD analyses, to obtain the aerodynamic loads to be used in topology optimization, is to define the flight envelope, from which the limit load factors will be taken. Based on these factors the lift coefficients can be obtained, and their corresponding angles of attack, through the XFLR5 graphs. This flight envelope consists of a diagram of the load factor (n) to which the aircraft is subjected, as a function of the speed (V) at which it travels. The load factor is measured in multiples of the gravity acceleration (g).

The flight envelope, without gust loads, is limited by aerodynamics, through the stall curve (by means of the $C_{L_{max}}$), by structural limit loads, in the form of maximum and minimum load factors, and by the dynamic pressure limit, which is expressed through maximum or dive velocity (V_{dive}) [15, 16].

In order to define the maximum and minimum load factors that can be expected for the UAV, the STANAG 4703 standard is used [17], intended for the certification of fixed-wing UAVs with a MTOW not exceeding $150kg$. According to this standard, for aircraft subject to symmetrical maneuvering, the maximum load factor shall be equal to or greater than 3.8g for positive loads and less than or equal to -1.5g for negative loads.

In addition to being dependent on flight operating conditions and maneuvers, the loads applied to the aircraft are also strongly related to external factors. The atmosphere behaves as a dynamic system, and gusts occur during flight. These imply a variation in the angle of attack and consequently in the value of the lift coefficient, so the load factor will also vary. For this reason, their effects on the loads experienced by the aircraft must also be included. For simplicity, gusts are often assumed to be symmetrical and vertical, so that the increment due to the gust load can be calculated directly.

The gust speed is extremely difficult to predict accurately, and is obtained from statistical flight data, taking into account the altitude range and flight conditions [15]. In the case under study, since it is a small aircraft, the values of gusts that it should support, depending on the flight altitude, are also present in the STANAG 4703 standard [17]. Once the increment in load factors from gusts that the aircraft may suffer is calculated, the flight envelope must be updated and contain new maximums and minimums for what the aircraft should withstand.

2.4. CFD Analyses

Computational Fluid Dynamics (CFD) can be seen as the use of numerical methods for the analyses of fluid flows. In the context of this article, the use of this resource aims to obtain the aerodynamic loads to which the aircraft will be subjected, and then use them in the topology optimization process. The software used in this process is Star-CCM+®, a commercial simulation software based on CFD, which allows high fidelity analyses of the aerodynamic characteristics of the UAV.

2.4.1 Validation

Before starting the study of the UAV, CFD analyses were performed on a NACA0012 airfoil, in order to validate the results obtained with the software and to justify the procedures for the CFD analysis of the UAV, both regarding mesh generation and the turbulence and transition models selected. To accomplish this purpose, wind tunnel data from NASA for the same airfoil [18] is used as a term of comparison.

In order to faithfully reproduce the tests performed in the wind tunnel, the CFD analysis was performed in two dimensions, in a plane that aims to replicate the center section of the wing used in the experimental tests. The selection of this plane is due to the fact that it is at this section that the pressure tapping points along the chord are found, and with which it was possible to obtain the graphs of pressure coefficient as a function of the chord percentage of the profile, which served as a term of comparison and validation for the analyses performed in CFD. The dimensions of the control area are equal to the length and height of the test volume of the wind tunnel where NASA performed the tests, as well as the remaining test parameters, such as the stagnation pressure, temperature, fluid velocity entering the test section, Reynolds number and angle of attack of the profile.

The Reynolds-Averaged Navier-Stokes (RANS) equations, which give an approximate time-averaged solution to the Navier-Stokes equations [19], are used for this work. These equations require a turbulence model to be solved. The choice fell on the $k-\omega$ model, a suitable model for low Reynolds number [20], where the boundary layer is relatively thick and the viscous sub-layer can be resolved. This is automatically coupled, by the software, to the turbulence model $k-\omega$ SST [21, 22].

In addition to a turbulence model, it is also necessary to select a transition model. The function of this is to predict the location of the transition from laminar to turbulent flow, if it exists, and whether it is a natural transition or a bypass transition, that is, a transition in which some of the steps of the natural transition process do not occur, due to external disturbances. In this case, the model used was $\gamma - Re_\theta$, compatible with unstructured meshes and built on local variables [23].

The boundary conditions were chosen in order to try to replicate the wind tunnel test conditions as much as possible. Therefore, a uniform inlet velocity was imposed, a zero pressure difference at the outlet compared to the stagnation pressure, a wall condition on the profile surface and a symmetry condition on the upper and lower surfaces of the test plane, in order to avoid the formation of boundary layer, since the tunnel where NASA performed the tests has a grid system that sucks the airflow close to the wall, in order to prevent the formation of boundary layer, and thus, reduce the wall effect as much as possible [24].

Next began the generation of the 2D, unstructured, hybrid mesh that is a mesh where each cell is a block, which leads to unlimited geometric flexibility and allows the most efficient use of computational resources for complex flows [25]. This type of mesh is more advantageous when dealing with

more complex geometries. The term hybrid mesh, on the other hand, is due to the use of more than one type of element, regular and irregular polygons. In order to better predict the flow behavior in the boundary layer near the solid wall, an unstructured mesh was generated with a mix of non-regular pentagons and hexagons in the generality of the test domain, and quadrilaterals in the region around the profile, called prism layer. Areas of further refinement were also created, one of rectangular shape around the entire profile and another in the wake region.

Once the mesh creation was finished, the convergence study was started. Between each analysis, a refinement ratio (r) was used, applied to all the mesh creation parameters. The formula used to calculate this refinement ratio is the following [22]

$$r = \left(\frac{N_1}{N_2}\right)^{\frac{1}{d}}, \tag{1}$$

where N_k is the number of mesh cells k and d is the number of dimensions of the problem under analysis. In this case, k takes the value of 1 for the most refined mesh and 2 for the least refined one, out of the two under study at each refinement, while d takes the value of 2, since the validation analyses were performed in two dimensions.

As mentioned above, in order to better capture the flow behavior in the boundary layer, prism layers were applied. The parameter that defines the thickness of the first prism layer and, consequently, how coarse or refined the mesh next to the profile is $y+$. This has not been defined directly, but rather through factors that are intrinsically linked to it, such as the total number of prism layers, the total thickness of these layers and the growth rate of these layers. The value of $y+$ must be carefully defined, because, depending on the turbulence and transition models chosen, it must be within a range of values (between 0 and 5) [26] that allows the correct application of the models.

In line with the primary objective of the validation analyses, the final step consists in comparing the parameters obtained through the CFD software used and those provided by NASA. In this case, this comparison was made through the C_p curves as a function of the chordwise percentage. The main objective of this comparison is the validation not only of the adopted models, but also of the chosen parameters and the mesh generation performed.

2.4.2 UAV CFD Analyses

Once the validation studies of turbulence and transition models, the parameterization of the analyses and the creation of the mesh are completed, the conditions are met to begin the study of the UAV.

The UAV wet surface is symmetric, so the analyses can be performed with only half of the aircraft, by using a symmetry condition in the longitudinal central plane.

The geometry and corresponding control volume were obtained using the geometric modeling program SolidWorks®, where a parallelepiped was created from which half the aircraft was subtracted, thus remaining with a positive mold of the aircraft, corresponding to the wet surface of the aircraft. Regarding the dimensions of the domain, it was taken into account that this is an analysis with subsonic flow, so the disturbance waves propagate in all directions, which implies larger dimensions of the domain, so that the selected boundary conditions do not negatively influence the results [27, 28].

The dimensions of the domain can be found in Fig.1, where c corresponds to the maximum chord of the aircraft (365 mm) and b corresponds to the total wingspan with the fuselage (1410 mm).

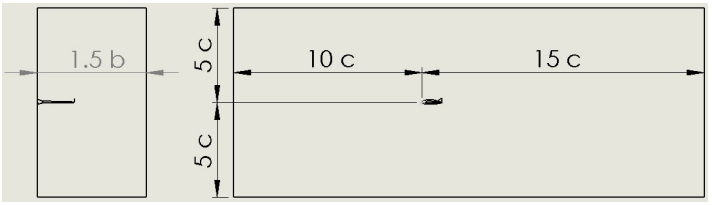

Figure 1: Domain dimensions as a function of the maximum chord (c) and wingspan (b)

Once the geometry is imported and the control volume is defined, it remains to define the boundary conditions and generate the surface and volume mesh, as the turbulence and transition models are the ones tested in the validation tests. For the inlet was assigned the condition of constant speed and equal to the cruise speed of the aircraft, 16.667 m/s, to the outlet was assigned constant pressure equal to the reference pressure, in this case the atmospheric pressure (101325 Pa), to the side faces was assigned symmetry condition, on the right side for representing only half of the aircraft and on the left side for simulating free flight condition without walls to delimit the domain. Finally, the UAV surface is considered a wall, being the interface between the solid and the fluid, and the upper and lower faces of the domain are considered inlet and outlet, respectively, for negative angles of attack, and vice-versa for positive angles of attack.

Similar to the procedure adopted in the validation studies, also in the case of the UAV a mesh convergence was performed in order to obtain a satisfactory set of parameters for mesh generation.

In this mesh convergence process three meshes with different refinements were generated. The first to be created was the coarsest and least computationally demanding. From there we went on to more refined meshes, having used the same method previously mentioned for the validation studies, the application of a refinement ratio (r) applied to all parameters of the generated mesh, between each of the cases.

Once the mesh convergence study was completed, a final mesh was obtained that was subsequently used in all the analyses performed on the UAV, for different angles of attack. This method was possible to be applied by keeping the geometry unchanged for all angles of attack and varying only the flow incidence angle. Thus it became feasible to always use the same mesh, speeding up the process.

After having generated the final mesh to be used in the analyses to remove the aerodynamic loads, it was time to pro-

ceed to three analyses with different angles of attack. These were intended to serve as starting points to perform a linear regression from the end points of C_L as a function of α. The need to elaborate this linear regression is due to the fact that the results obtained with Star-CCM+® may diverge from those obtained with XFLR5. In the case under study, some of the reasons that may lead to this difference are the non-use of winglets in the XFLR5 analyses, or the differences in the fuselage profile, which was generated in XFLR5 for the XFLR5 studies, and in SolidWorks® for the model applied in the Star-CCM+® tests. Since the reliable geometry corresponding to the final UAV is that generated in SolidWorks®, the results obtained through Star-CCM+® were the ones accepted as being the most realistic and reliable. Therefore, with the linear regression it becomes possible to achieve the value of the new angles of attack for the cruise and extreme conditions of the flight envelope previously presented, that is, the cases of +3.8g and -1.5g.

The UAV analyses were all started in steady state, but in order to achieve satisfactory convergence for the lift coefficient, it was decided to change one of the physical parameters of the analysis and switch to unsteady state. The non-convergence in steady state can be related to some location of the flow where there is no stationarity, and thus, the solution does not converge. The location of these points responsible for the phenomenon, in the UAV under development, could be at the point where the transition from laminar to turbulent regime takes place, on the upper surface of the fuselage and at certain points located along the wingspan.

After performing the three simulations, for cruise conditions and load factors of -1.5g and +3.8g, according to the data obtained from XFLR5, we proceeded to linear regression and to the calculation of the new angles of attack to be used in the final analyses, which are in line with the values obtained in Star-CCM+®.

Similarly to what was done in the analyses for the linear regression, it was also chosen in these final analyses to start the process in steady state and, in order to obtain the convergence of the parameters, move to unsteady state when the residuals of the steady state analysis stabilize.

Once the analyses were finished and having convergence in all parameters, a comparison was made between the values obtained with the CFD software and those obtained with the XFLR5, as well as calculated the new estimate of the maximum flight time. The pressure distributions, resulting from the final analyses, were subsequently used to import the aerodynamic loads in the topology optimization.

2.5. Topology Optimization

Topology optimization is a mathematical and computational method that allows, through the distribution of material in a structure without prior topology, or with freedom in it, to minimize the weight and material used and maximize the performance of the system of which it is part [29]. The optimization is done taking into account an allowed design space and the constraints and loads to which the structure is subjected.

The CAD model imported into the software responsible for the topology optimization, Altair HyperWorks®, was created using the geometric modeling software SolidWorks®. This was the same that was used to do the subtraction process that originated the enclosure with the wet surface used in the CFD analyses. It was created based on the constraints imposed by the internal components and according to the measurements obtained in the initial design and configuration of the wing. In Fig.2 a view of this model is depicted.

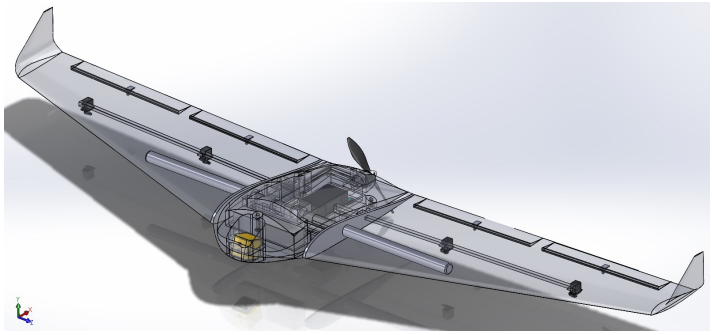

Figure 2: CAD obtained with SolidWorks®

Once the geometry has been imported, a mesh that is refined enough to provide a correct discretization and accurately describe the shape of the aircraft must be generated. This can have different degrees of refinement, depending on the area where it is applied, i.e. whether it is a part that is intended to be optimized or not.

Once the geometry has been introduced, the separation into different regions made, and the mesh generated, the loads that will give rise to the optimization process can then be applied. These are applied at isolated points or distributed over the nodes of a given surface of the generated mesh. In this case study, the masses of the internal components were applied, the materials and respective characteristics of the various UAV components were defined, and the aerodynamic loads from the CFD analyses were imported. It is also necessary to fix nodes of the geometry, so that the forces can be applied. In this case, it was chosen to fix the fuselage nodes that are in contact with the carbon spar, for being the element with the highest stiffness of the assembly, and those that are in contact with the fitting pins of the side profiles located between the fuselage and the wings.

The last step to take before initializing the structural analysis and subsequent topology optimization, is to create groups with selected contact surfaces, in order to transmit forces and displacements between the different components that constitute the complete geometry under study.

Then, the setup for the optimization is done, in which various constraining parameters can be entered, based on which the analysis will run. In the context of the UAV development project in question, the goal of the topology optimization is to reduce the percentage of material, a percentage that is relative to the volume occupied by the aircraft. Therefore, minimum mass and maximum stress limit values, which the aircraft should not exceed and to which its components should not be subjected, should be introduced.

After the software runs the optimization, the user has the ability to visualize the shape of the structure obtained in the process of optimal material distribution and, with this, try to reproduce the shape achieved with the aid of CAD software, for example.

3. Results

3.1. Conceptual Design

In the conceptual design phase, the MTOW was calculated, and a value of 10.9293N was obtained. The values of the remaining parameters used to calculate the Design Point, by applying the constraints mentioned in Sec. 2.2, are presented in Tab.1. From the analysis of the Design Point graph, a $P/W = 3.74325\ W/N$ constrained by the climb stage and a $W/S = 44.3064\ N/m^2$ limited by stall speed were obtained. Using these values, together with the MTOW, a wing area of $0.2467\ m^2$ was obtained.

Table 1: Parameters and properties considered in the initial design.

Parameters and Properties	Dimension
MTOW $[N]$	10.9293
Cruise altitude (h_{cr}) $[m]$	20
Air density (ρ_{cr}) $[kg/m^3]$	1.225
Air temperature (T_{cr}) $[^{\circ}C]$	20
Cruising Speed (V_{cr}) $[m/s]$	16.667
Viscosity (μ_{cr}) $[Pa \cdot s]$	0.000018134

3.2. Preliminary Design

3.2.1 Wing Profile Selection

The process of choosing the wing profile was based on the analysis of the parameters discussed in chapter 2.3.1. In the end, based on the analyses carried out in XFLR5, the choice fell on the MH 81, for being the one that demonstrated a more homogeneous behavior, standing out in a positive way regarding the lift coefficient and the stall behavior, and presenting a rather neutral behavior in the remaining evaluations.

3.2.2 Wing Configuration

Using the value of the wing area defined in the previous sub-section, together with the constraint of a wingspan of 1200 mm and the selection of some parameters stated in the Sec. 2.3.2, according to the references present therein and for a flying wing aircraft, the parameters summarized in Tab.2 were obtained. Note that the values shown in Tab.2, relate only to the wings, not taking into account the fuselage, which was created in XFLR5, due to the impossibility of uploading the one generated in SolidWorks®. From the analyses performed on the complete aircraft in XFLR5, with the characteristics listed above, resulted the data presented in Tab.3. With all this information, is already possible to define the stall speed which is $7.22 m/s$.

Table 2: Wing configuration parameters.

Parameter	Dimension
Wing Span (b) [mm]	1200
Root chord (c_{root}) [mm]	293.66
Tip chord (c_{tip}) [mm]	117.46
Mean chord $(\overline{c})$ [mm]	218.15
Taper ratio (λ)	0.4
Sweep angle (Λ) $[^{\circ}]$	15
Aspect ratio (AR)	5.839

Table 3: Data regarding the aircraft study in XFLR5.

Data	Value	Data	Value
$C_{L_{cr}}$	0.237	C_{L_α} $[/^{\circ}]$	0.0648
$C_{L_{max}}$	1.260	$(C_L/C_D)_{cr}$	15.70
$C_{D_{cr}}$	0.015	$(C_L/C_D)_{max}$	19.788
C_{D_0}	0.0138	$(C_L^{3/2}/C_D)_{cr}$	7.65
$C_{M_{cr}}$	-0.0532	$(C_L^{3/2}/C_D)_{max}$	14.465
C_{M_0}	-0.0494	$\alpha_{C_{L_{max}}}$ $[^{\circ}]$	15
α_{cr} $[^{\circ}]$	0.23		

3.2.3 Static Stability Analysis

Regarding longitudinal stability, a negative C_{M_α} and a value of C_{M_0} of -0.0494 were estimated, i.e., ensuring longitudinal stability. A rearrangement of the internal components in the fuselage was also performed in order to move the CG of the UAV and obtain a static margin of 0.077, situated within the desired value range of 0.02 to 0.08.

Turning now to the directional stability analysis, the yaw coefficient was calculated, with previously obtained data, such as $C_{L_{cr}}$, AR, Λ and $x/\overline{c}$, where $\overline{c}$ is the mean chord and x is the distance between the center of gravity and the aerodynamic center. Upon completion of the calculation, a yaw coefficient value of 0.0013 was obtained, meeting the requirement that it must be positive.

3.2.4 Flight Envelope

Following the methodology presented in chapter 2.3.4, the flight envelope was obtained considering a dive speed of 25.0 m/s, a cruise speed of 16.667 m/s and a stall speed of 7.223 m/s. Going by the information contained in the STANAG 4703 standard, the maximum load factor for positive loads is +3.8g and for negative loads is -1.5g.

However, the aircraft may suffer effects caused by weather and atmospheric conditions that lead to more demanding conditions. Therefore, the effect of gusts must be taken into account, which leads to a maximum load factor for positive and negative loads of, respectively, 9.5765 and -7.5765, these when not considered any design factor that multiplies these values, introducing a safety margin.

3.3. CFD Analyses

3.3.1 Validation

The first validation analyses were intended to perform a mesh convergence, which was successful and achieved with only two refinements, verifying relative errors in lift and drag coefficients below 5%.

In all three cases, for an angle of attack equal to -4°, 0° and 4°, the curves from the analyses carried out, follow the curves generated by the data acquired from the NASA study almost perfectly, as it can be seen in Fig.3, corresponding to the analysis with an angle of attack of 4°. Small visible deviations can be justified with errors associated with CFD analyses, which do not represent at 100% the test conditions experienced in the wind tunnel used by NASA. These differences in the value of C_p along the chord are more visible in the case of analyses with angle of attack equal to -4° and 4°, more sensitive to slight changes in the flow parameters, since , being a symmetrical profile, at 0°theoretically there is no lift creation or pressure difference between the lower and upper surfaces, being this analysis less susceptible to errors. Even so, these verified deviations take the form of curve displacements and not peaks at certain points, so they must be associated with disparities in the test parameters and not with domain discretization or model applicability errors. This suggests that the analyses provide reliable data and are worthy of validating the adopted process.

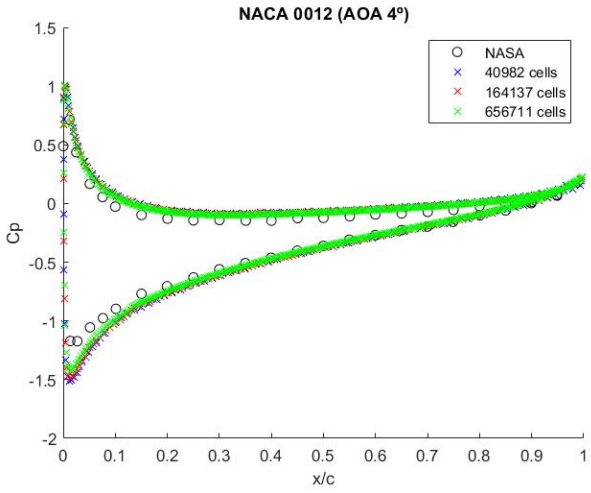

Figure 3: Pressure coefficient as a function of chord percentage for $\alpha = 4°$.

3.3.2 UAV CFD Analyses

Similar to the procedure adopted in the studies for validation, a mesh convergence was also performed in the case of the UAV. In this process three meshes with different refinements were generated, from the coarsest to the most refined, with refinement ratios of 1.5. In Fig.4 is a close-up of the mesh generated in the plane of symmetry of the aircraft, for the entire domain, where the regions of localized refinement can be seen, around the UAV and in the region of the wake generated by it. In this case, it corresponds to the final and most refined one.

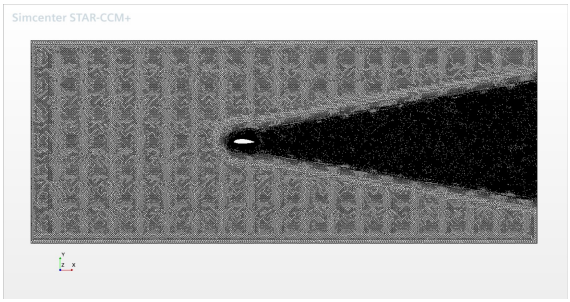

Figure 4: More refined convergence mesh

Tab.4 contains the data analyzed in the mesh convergence process for the UAV.

The criterion for acceptance of convergence was the 5% relative error, also used in the validation process. This criterion was met in the case of the lift coefficient, however, for the drag coefficient it was not possible to achieve. This result was to be expected, partly because it is notoriously more demanding to achieve convergence for drag. Therefore, it was decided to accept the 8.333%, since to decrease this value would already require a great deal of refinement and available computational power.

The mesh was then given as converged and accepted. It was therefore this mesh with 7159918 elements that was subsequently used in all the analyses done on the UAV, for different angles of attack.

During the analyses performed for mesh convergence, it was found that the results obtained from Star-CCM+® were quite disparate from those calculated with XFLR5. As a way to understand this discrepancy in the C_L and C_D values, a linear regression was performed to obtain the new angle of attack values that would lead to C_L values similar to those needed to perform simulations taking into account the +3.8g and -1.5g load factors. Note that these were the load factor values used for limit situations, as they already correspond to angles of attack relatively close to those of stall, so before the aircraft reaches the load factors calculated taking gusts into account, it would go into stall. That is, the aerodynamic limits would be reached before the structural limits could be reached.

Consulting the values of the relative differences obtained, could be concluded that the linear regression performed previously, with the objective of finding the new angles of attack that would lead to the values of C_L corresponding to the loads in question, was successfully performed, because the magnitude of the differences between both programs is quite low. These were therefore the final analyses from which the aerodynamic loads to be applied in the topological optimization were taken.

3.4. Topology Optimization

In order to get to know the program better and to define the necessary steps to elaborate a correct setup for the fi-

Table 4: Mesh convergence data for UAV.

Mesh Type	**Number of Cells**	C_L [-]	**Relative Error** [%]	C_D**[drag counts]**	**Relative Error** [%]
Coarse	722130	0.0880	6.0	103.44	60.6
Intermediate	2095696	0.0809	2.5	69.78	8.3
Refined	7159918	0.0830	-	64.41	-

Table 5: Comparison of the results obtained with XFLR5 and Star-CCM+®.

Flight Condition	**Software**	α [°]	C_L	**Diff** [%]	C_D	**Diff** [%]
-1.5 G	XFLR5	-7.3	-0.355	3.27	0.0512	7.91
	Star-CCM+®	-6.893	-0.367		0.055596	
Cruise	XFLR5	0.23	0.237	0.42	0.0156	0.29
	Star-CCM+®	1.078	0.236		0.015555	
+3.8 G	XFLR5	8.75	0.900	4.76	0.0597	0.69
	Star-CCM+®	9.548	0.945		0.060112	

nal topology optimization of the UAV fuselage, a preliminary optimization was performed. This targeted the fuselage and followed all the steps described in chapter 2.5. The main difference to the final optimization is that in the preliminary optimization, only the loads of the internal components and the mass of the fuselage itself were taken into account in the process of preparing the optimization.

Since the results obtained with this analysis were not intended to have quantitative value, being only a test, the constraints imposed on the optimization were quite conservative and less demanding than those to be applied in the final analysis. The maximum allowed stress value corresponds to the yield stress of the PLA, multiplied by a safety factor of 1.5, while the minimum value of mass that the fuselage could reach was 2 kg. Fulfilling its goal, the optimization went smoothly and returned a simplified UAV fuselage geometry.

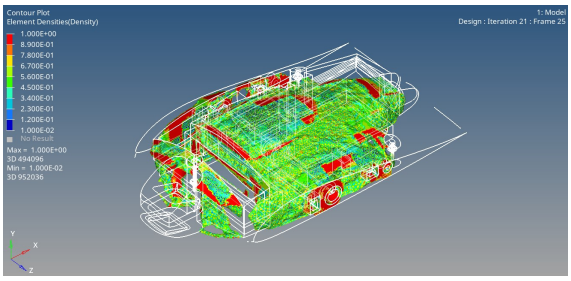

Figure 5: Geometry resulting from preliminary topology optimization

From the analysis of the Fig.5, where only the elements of the mesh with more than 50% of relative density appear, it can be concluded that even for an extremely conservative minimum mass value, such as 2 kg, much of the outermost material of the fuselage is dispensable, and the internal structure can be greatly simplified and the outer surface kept only with a kind of shell, in order to meet the aerodynamic requirements arising from the development of the UAV.

Unfortunately, in the time available for this work, it was not possible to obtain the results of the final topology optimization. Still, the whole setup is ready to run and then be able to conclude whether the mass objectives can be achieved with the geometry and requirements presented.

4. Conclusions

Following standard aircraft development methodology, the design and study of an UAV for motorsport surveillance in a racetrack environment was carried out. This methodology had to undergo minor adjustments, given the unusual geometry of the aircraft in question, yet the main steps were followed.

In an initial phase, the MTOW of the aircraft was calculated, through a careful choice of materials and components for the aircraft, followed by the Design Point, which allowed to proceed to a preliminary design of the UAV. With the aid of CAD software, this concept aircraft was designed, taking into account the design constraints, the dimensions obtained previously, the selected geometry and the component distribution resulting from a stability analysis.

With the geometry designed, the CFD analyses process was started, in order to obtain the aerodynamic loads to be used in the subsequent topology optimization.

It is important to note that the topology optimization process is still in progress, so the results are not available yet for presentation in the present version of this paper.

Acknowledgements

To Althima-Engineering Software Solution, Lda and Altair Engineering Inc. for providing an Altair license allowing for the development of the CAE simulation conducted during this work.

References

[1] R. Karimi Kelayeh and M. H. Djavareshkian. Aerodynamic investigation of twist angle variation based on

wing smarting for a flying wing. *Chinese Journal of Aeronautics*, 34(2):201–216, 2021.

[2] L. Wang, N. Zhang, T. Yue, H. Liu, J. Zhu, and X. Jia. Three-axis coupled flight control law design for flying wing aircraft using eigenstructure assignment method. *Chinese Journal of Aeronautics*, 33(10):2510–2526, 2020.

[3] T. C. Corke. *Design of Aircraft*. Prentice Hall, Upper Saddle River, NJ, USA, 2003.

[4] D. P. Raymer. *Aircraft Design: A Conceptual Approach*. AIAA, 5^{th} edition, 2012.

[5] P. Edi, N. Yusoff, and A. Ahmad-Yazid. The design improvement of airfoil for flying wing uav. *WSEAS Transactions on Applied and Theoretical Mechanics*, 3:809–818, 09 2008.

[6] A. Alsahlani and T. Rahulan. Aerofoil design for unmanned high-altitude aft-swept flying wings. *Journal of Aerospace Technology and Management*, 9:335–345, 08 2017.

[7] XFLR5. `http://www.xflr5.tech/xflr5.htm`. Accessed: 10/07/2020.

[8] M. Drela. Xfoil: An analysis and design system for low reynolds number airfoils. In T. J. Mueller, editor, *Low Reynolds Number Aerodynamics*, pages 1–12, Berlin, Heidelberg, 1989. Springer Berlin Heidelberg.

[9] A. Lennon. *Basics of R C Model Aircraft Design: Practical Techniques for Building Better Models*. Air Age Media Inc., East Ridge, TN, USA, 1996.

[10] M. H. Sadraey. *Aircraft Design: A Systems Engineering Approach*. John Wiley & Sons, Ltd, Chichester, UK, 2013.

[11] J. Hall, K. Mohseni, D. Lawrence, and P. Geuzaine. Investigation of variable wing-sweep for applications in micro air vehicles. 4:6–9, 09 2005.

[12] A. J. Keane, A. Sóbester, and J. P. Scanlan. *Small Unmanned Fixed-wing Aircraft Design: A Practical Approach*. John Wiley & Sons, Ltd, Chichester, UK, 2017.

[13] J. D. Anderson. *Fundamentals of Aerodynamics*. McGraw-Hill, 5th edition, 2010.

[14] Z. Chen, M. Zhang, Y. Chen, W. Sang, Z. Tan, D. Li, and B. Zhang. Assessment on critical technologies for conceptual design of blended-wing-body civil aircraft. *Chinese Journal of Aeronautics*, 32(8):1797–1827, 2019.

[15] T. H. G. Megson. *Aircraft Structures for Engineering Students*. Butterworth-Heinemann, Oxford, UK, 4th edition, 2007.

[16] F. Perini. Structural design, manufacturing and testing of a new wing for the csir's modular uas in composite materials. Master's thesis, University of Bologna, 2012.

[17] NATO. *STANAG 4703 Light Unmanned Aircraft Systems Airworthiness Requirements*. 2nd edition, 2016.

[18] C. L. Ladson, A. S. Hill, and W. G. Johnson. Pressure distributions from high reynolds number transonic tests of an naca 0012 airfoil in the langley 0.3-meter transonic cryogenic tunnel. Technical Report 100526, NASA, December 1987.

[19] J. H. Ferziger and M. Peric. *Computarional Methods for Fluid Dynamics*. Springer, Germany, 2002.

[20] A. Tomboulides, S.M. Aithal, P.F. Fischer, E. Merzari, A.V. Obabko, and D.R. Shaver. A novel numerical treatment of the near-wall regions in the k class of rans models. *International Journal of Heat and Fluid Flow*, 72:186–199, 2018.

[21] Y. You, F. Seibold, S. Wang, B. Weigand, and U. Gross. Urans of turbulent flow and heat transfer in divergent swirl tubes using the k- sst turbulence model with curvature correction. *International Journal of Heat and Mass Transfer*, 159:120088, 2020.

[22] T. Rocha. Numerical and experimental study of wing tip endplates of a formula student car. Master's thesis, Instituto Superior Técnico, 2020.

[23] F. Menter, R. B. Langtry, S. Likki, Y. Suzen, P. Huang, and S. Völker. A correlation-based transition model using local variables—part i: Model formulation. *ASME J. Turbomach*, 128, 07 2006.

[24] C. L. Ladson and E. J. Ray. Evolution, calibration, and operational characteristics of the two-dimensional test section of the langley 0.3-meter transonic cryogenic tunnel. 1987.

[25] J. Tu, G. H. Yeoh, and C. Liu. *Computarional Methods for Fluid Dynamics*. Butterworth-Heinemann, Oxford, UK, 2013.

[26] M. Ariff, M. Salim, and S. C. Cheah. Wall y+ approach for dealing with turbulent flows over a surface mounted cube: Part 2 - high reynolds number. 01 2009.

[27] F. Goetten, D. F. Finger, M. Marino, C. Bil, M. Havermann, and C. Braun. A review of guidelines and best practices for subsonic aerodynamic simulations using rans cfd. In *Asia Pacific International Symposium on Aerospace Technology*, Gold Coast, Qld, Australia, 2019.

[28] B. Gossant. Chapter 4 - solid propellant combustion and internal ballistics of motors. In Alain Davenas, editor, *Solid Rocket Propulsion Technology*, pages 111–191. Pergamon, Amsterdam, 1993.

[29] O. Sigmund and K. Maute. Topology optimization approaches. *Structural and Multidisciplinary Optimization*, 48:1031–1055, 2013.